THE PLANT CELL

The Plant Cell, 2025, **00**, koaf183

https://doi.org/10.1093/plcell/koaf183
Advance access publication xx xx 0000
Research Article

The wheat transcription factor Q functions in gibberellin biosynthesis and signaling and regulates height and spike length

Pan Liu,[1,†] Shulin Xue,[2,*,†] Jizeng Jia,[1,†] Guangyao Zhao,[1] Jie Liu,[3] Yanzhen Hu,[1] Cuizheng Kong,[1] Dong Yan,[1] Huan Wang,[2] Xu Liu,[1,*] Zefu Lu,[1,*] Lifeng Gao[1,*]

[1]State Key Laboratory of Crop Gene Resources and Breeding, Institute of Crop Sciences, Chinese Academy of Agricultural Sciences, Beijing 100081, China
[2]State Key Laboratory of Crop Stress Adaptation and Improvement, School of Life Sciences, Henan University, Kaifeng, Henan 475004, China
[3]State Key Laboratory for Agrobiotechnology and Key Laboratory of Crop Heterosis and Utilization (MOE) and Beijing Key Laboratory of Crop Genetic Improvement, China Agricultural University, Beijing 100193, China
*Author for correspondence: gaolifeng@caas.cn (L.G.); luzefu@caas.cn (Z.L.); liuxu01@caas.cn (X.L.); xsl@vip.henu.edu.cn (S.X.)
†These authors contributed equally to this work.
The author responsible for distribution of materials integral to the findings presented in this article in accordance with the policy described in the Instructions for Authors (https://academic.oup.com/plcell/pages/General-Instructions) is: Lifeng Gao (gaolifeng@caas.cn).

Abstract

The Q gene is a key domestication gene in wheat (*Triticum aestivum*) that regulates free-threshing habit, spike morphology, height, and other critical agronomic traits. However, the precise molecular mechanisms underlying its function remain unclear. In this study, we identified a Q allele with a missense mutation (G to A) in the fifth exon of the Q gene, resulting in reduced plant height and spike length. Further investigation revealed that this mutation causes a Gly-229-Ser amino acid substitution, which enhances Q protein stability. Furthermore, we discovered that Q directly binds to the promoter region of *Gibberellin 3-oxidase 2* gene (*Ta*GA3*ox2*) and represses its expression. Moreover, Q interacts with both REDUCED HEIGHT1 (RHT1) and GIBBERELLIN INSENSITIVE 2 (*Ta*GID2), which may disrupt GID2-triggered RHT1 degradation. Collectively, these findings reveal the dual roles of Q in regulating both GA biosynthesis and signaling, providing insights into the molecular mechanisms through which Q modulates plant height and spike length in wheat.

Introduction

The Q gene plays an important role in the domestication of wheat, as it governs traits such as the fully tough rachis, free-threshing, and spike density. In addition to those domestication traits, Q also regulates important agronomic traits such as height, spike length, yield, quality, and heading date (Muramatsu 1963 ; Simons et al. 2006; Zhang et al. 2011, 2022; Xie et al. 2018; Xu et al. 2018; Zhao et al. 2018). However, the studies on the underlying molecular mechanisms remain to be elucidated.

The Q gene encodes an APETALA2 (AP2) transcription factor (AP2L5) that contains 2 tandem AP2 domains (Simons et al. 2006). Its N-terminal EAR motif (LDLNVE) can recruit the transcription co-repressor TOPLESS (*Ta*TPL) to achieve transcriptional inhibition (Liu et al. 2018). A substitution of G to A at position 2,123 in the eighth exon leads to a single V329I amino acid change and a synonymous mutation at the microRNA172 (miR172) target site in the tenth exon, resulting in the hyper-functionalization of 5A*q* to 5AQ (Simons et al. 2006; Zhang et al. 2011). The hexaploid wheat genome carries 3 functionally differentiated homologous copies of Q gene, with both 5AQ and 5D*q* expected to produce functional Q/q proteins, while 5B*q* is classified as a pseudogene encoding truncated proteins lacking the AP2 DNA-binding domain (Zhang et al. 2011). Q might regulate the free-threshing trait of wheat by suppressing the expression of lignin-related genes such as *Knotted Arabidopsis thaliana7* (*Ta*KNAT7), *Ta*MYB46, and *Bell1-like homoeodomain* (*Ta*BLH6), thereby reducing cell wall hardness (Zhang et al. 2020). Furthermore, Q interacts with Lax Panicle1 (*Ta*LAX1) to antagonistically regulate the expression of the lignin synthesis gene *Ta*KNAT7-4D. Consequently, overexpression of *Ta*LAX1 leads to a spelt-like spike resembling *q* (He et al. 2021).

Studies have primarily focused on the miR172 pathways to investigate how Q regulates height and spike length (Zhang et al. 2011; Debernardi et al. 2017; Greenwood et al. 2017; Liu et al. 2018; Xu et al. 2018). Mutations in the miR172 binding site of Q^{c}, Q^{c5}, and 5D*q*′ (*Rht23*) resulted in dwarfism, compact spike, increased 1000-grain weight, grain protein content, and bread-making quality (Chen et al. 2015; Xu et al. 2018; Zhao et al. 2018; Guo et al. 2022). Additionally, mutations in the AP2 domain also impact its function. *mq*194, *q*′ and Q^{s1} with mutations in the AP2-R1 domain of Q exhibit a morphological switch from square spikes to spelt spikes and increased height (Simons et al. 2006; Madsen and Brinch-Pedersen 2020; Chen et al. 2022). Furthermore, mutations or insertion of a 161 bp fragment in the fifth exon of *Q-e5t* and Q^{t} led to the deletion of the AP2-R2 domain resulting in increased spike length and height (Jiang et al. 2019; Zhang et al. 2022).

Gibberellins (GAs) are vital in regulating seed germination, stem elongation, epidermoid development, flower organogenesis, and fruit ripening (Binenbaum et al. 2018; Wu et al. 2021). GA synthesis involves the conversion of geranylgeranyl pyrophosphate into kaurene and GA_{12} in the plastids and endoplasmic reticulum

Received April 01, 2025. Accepted June 23, 2025.

(Sun et al. 1992; Yamaguchi et al. 1998; Helliwell et al. 2001; Fleet et al. 2003). Subsequently, GA_{12} is converted to GA_1 through the early-13-hydroxylation pathway, while GA_4 is synthesized through the non13-hydroxylation pathway. These conversions are catalyzed by GA13 oxidase (GA13ox), GA20 oxidase (GA20ox) and GA3 oxidase (GA3ox) in the cytoplasm (Chiang et al. 1995; Phillips et al. 1995; Varbanova et al. 2007). To date, over 130 different GAs have been identified in plants. Among these, GA_4 is a bioactive 13-H GA, while GA_1 is less active 13-OH GA (Magome et al. 2013).

In terms of GA signal perception and transduction, active GA binds to its receptor GID1 (Gibberellin Insensitive Dwarf1), facilitating the interaction between GID1 and the growth-repressing transcription factor (TF) DELLA. This interaction enables DELLA to be ubiquitinated by the SCF (Skp, Cullin, F-box) ubiquitin ligase complex, leading to its subsequent degradation in the 26S proteasome (Sasaki et al. 2003; Murase et al. 2008; Shimada et al. 2008; Harberd et al. 2009). This degradation process relieves the growth-restraining effects of DELLA proteins and allows for GA-mediated growth and development (Dill et al. 2004; Fu et al. 2004; Ueguchi-Tanaka et al. 2005). Defects in GA biosynthesis and/or signaling pathways lead to reductions in height and silique length (Hu et al. 2008).

The "Green Revolution" in rice and wheat is closely linked to GA, as mutations in gibberellin-related genes result in reduced height and enhanced yield (Peng et al. 1999; Sasaki et al. 2002). *Rht1* encodes a DELLA protein, and its dominant mutations (*Rht-B1b* and *Rht-D1b*) confer the DELLA protein resistant to degradation, resulting in the accumulation of DELLA protein in wheat. This accumulation ultimately leads to the semi-dwarf phenotype (Peng et al. 1999; Zhang et al. 2014). In barley, disruptions in the targeting of miR172 to *HvAP2* can lead to a decreased responsiveness to GA-induced stem growth (Patil et al. 2019). However, the relationship between Q, which is involved in height and spike length, and the GA pathway is still poorly understood.

In this study, we characterized a Q mutant harboring a G229S mutation caused by a G to A substitution, which exhibited reduced height and spike length. Through investigating this Q allele, we elucidated that Q could negatively regulate GA biosynthesis by directly binding to the GCC motifs in the *GA3ox2* promoter and may also block GA signaling by competitively interacting with GID2 and suppressing RHT1 degradation in wheat.

Results

Identification of an allele of Q

By screening the ethyl methane sulfonate mutant library of a Chinese wheat landrace Wangshuibai (WSB), we identified a mutant *mw164* exhibiting reduced height and spike length (Fig. 1A; Supplementary Fig. S1, A and B). Compared with WSB, the peduncle length, height, spike length and spikelet number per spike of *mw164* were reduced by 13.4%, 18.4%, 39.5%, and 14.29% (Fig. 1, B and C; Supplementary Fig. S1, C and D, Table S1), respectively, while the spikelet density was increased by 44.8% (Supplementary Fig. S1E). Microscopic analysis revealed that the shortened peduncle and spike in *mw164* were primarily due to a reduction in cell lengths rather than a decrease in cell counts (Fig. 1, D and E).

In order to identify the gene responsible for the reduced height and spike length, we conducted crosses between *mw164* and 2 different wheat cultivars, WSB and Nanda2419 (ND2419), which exhibit distinct spike length. The spike length in the 242 plants of the (*mw164* × ND2419) F_2 population and the 102 plants of the (*mw164* × WSB) BC_2F_2 population both displayed trimodal distribution (Supplementary Fig. S1, F and G), implying that a single locus regulates the spike morphologies in a dose-dependent manner. Bulked segregant analysis initially mapped this locus to the region harboring *Xbarc319* on chromosome 5A (Supplementary Fig. S1H), which was named *QSpl-5A*. The log of the odds value of this locus peaked at *Xcaps-Q*, a cleaved amplified polymorphic sequence (CAPS) marker designed from a G/A single nucleotide polymorphism (SNP) in the 3′-UTR region of the *Q* (*AP2L5*) gene (Supplementary Fig. S1I).

By genotyping of the individuals, *Qspl-5A* was further narrowed to a region flanked by *Xbarc319* and *Xgwm595* in the *mw164* × ND2419 F_2 population (Supplementary Fig. S1J). To identify the responsible gene in this region, we re-sequenced WSB and *mw164* using a BGISEQ-500 platform with 12-fold coverage. Seven polymorphic CAPS/dCAPS/SNP markers were developed in this region (Supplementary Fig. S2A). A genetic map was constructed using the 102 BC_2F_2 plants derived from *mw164* × WSB (Supplementary Fig. S2B). With the help of the critical recombinants (Supplementary Table S2), *Qspl-5A* was finely mapped to a 1.41 Mb interval flanked by *SNP65131* and *CAPS65272*, which contained 33 high-confidence genes according to Chinese Spring (CS) reference genome v2.1 (Fig. 1F; Supplementary Table S3). There are 20 SNPs located within the *SNP65131-CAPS65272* interval between WSB and *mw164*. Of these, 19 SNPs are situated within the intergenic regions, while only SNP11 (G to A) is located within the fifth exon of *TraesCS5A03G1116700* (*Q*) (Supplementary Table S4). The mutation from G to A (Fig. 1F) results in Gly changed to Ser at position 229 (G229S) in the AP2-R2 domain of Q (Supplementary Fig. S3A). Subsequently, a diagnostic marker *Kasp-Q* was developed based on the G/A SNP (Supplementary Fig. S3B) and utilized to examine its linkage with spike length in 2 separated populations. All the (*mw164* × ND2419) F_2 and (*mw164* × WSB) BC_2F_2 individuals exhibiting mutant phenotypes carried the site mutation (Fig. 1, G and H; Supplementary Table S5). These findings suggest that the mutated Q^{G229S} is a potential candidate gene responsible for the reduced height and spike length.

Q^{G229S} reduces height and spike length by enhancing the protein stability and homodimer formation

To further confirm the role of the G229S mutation in reducing height and spike length of *mw164*, we performed guided editing to create the exact same G to A mutation in Q gene in wheat cultivar Kenong199 (KN199). The height and the spike length of *PE-*Q^{G229S} lines were decreased by 17.0% and 32.1%, respectively (Fig. 1, I to L; Supplementary Table S1), which is consistent with mutant phenotype of *mw164*. We also checked whether the mutation affected gene expression and found no significant difference in the expression level of Q between young spikes of *mw164* and WSB (Supplementary Fig. S3C). Additionally, protein structure predictions for the Q and Q^{G229S} proteins indicated that the amino acid change at position 229 within the AP2-R2 domain altered the tertiary structure but did not affect the secondary structure (Supplementary Fig. S3, D and E), suggesting the mutation may affect protein level and/or functions but not transcriptional level.

We then also overexpressed the Q and Q^{G229S} driven by the *Ubiquitin* promoter in wheat cultivar Kenong199 (KN199), respectively. Both *Q*/Q^{G229S}overexpression lines (*pUbi*:Q and *p*Ubi:Q^{G229S}) showed reduced height and spike length, while the

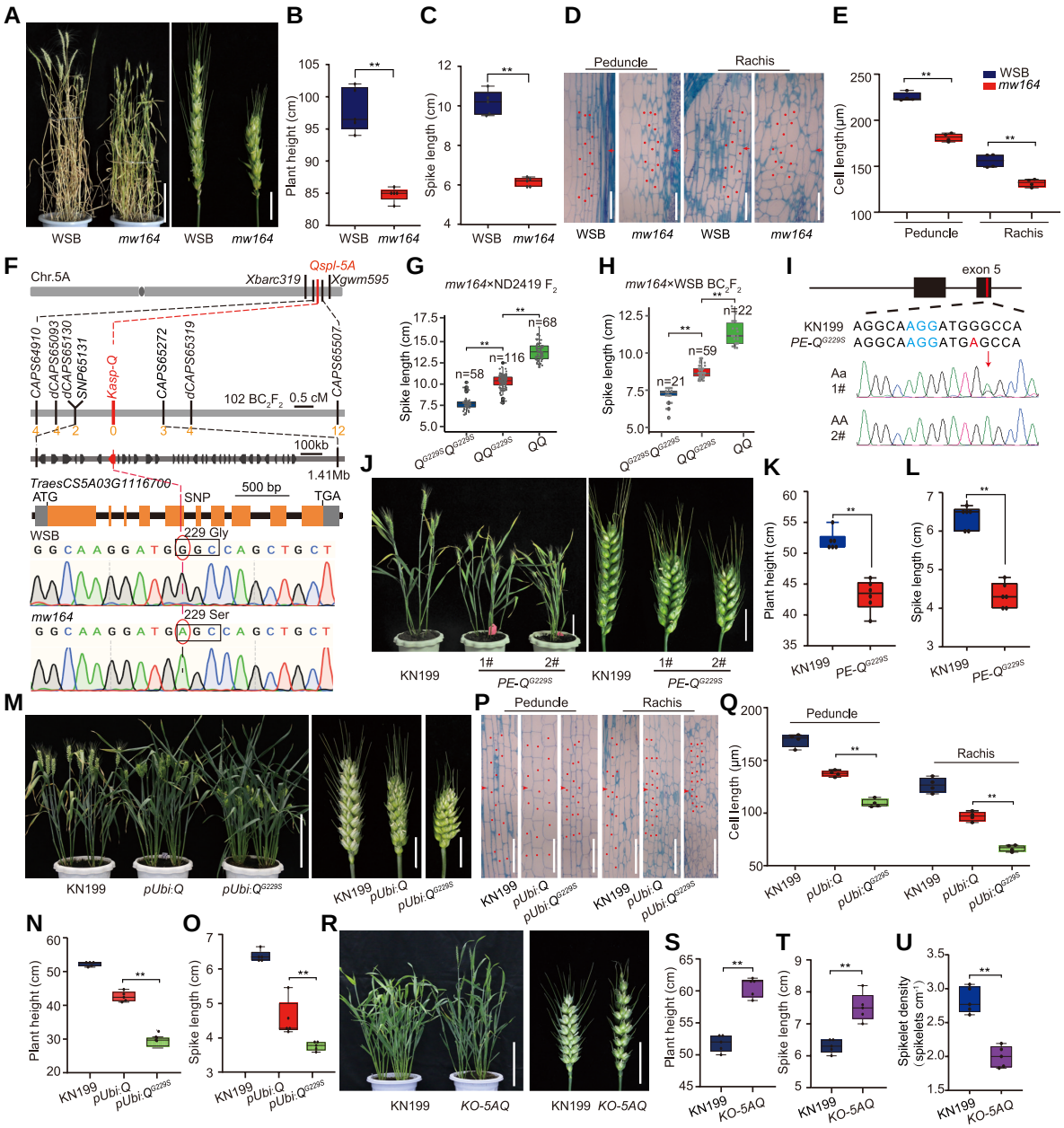

Figure 1. Phenotype characterization of *mw164* mutant and map-based cloning of *QSpl-5A*. **A)** Phenotypes of the height and spike length in WSB and *mw164* mutant at the milky stage. Scale bar, 20 cm (left) and 2 cm (right). **B, C)** Statistical analysis of height and spike length in WSB and *mw164* mutant. The values are means ± SD ($n = 5$). WSB, the Chinese wheat landrace WSB. **D)** Median longitudinal sections through the rachises and peduncles at the booting stage (W8.5-W9) in WSB and *mw164* mutant. Scale bar, 200 μm. Arrowheads indicate the proximal end of the epidermal. The red dots mark the 3rd to 5th parenchyma selected for quantification analysis. **E)** Average cell length of peduncle and rachis in the WSB and *mw164* mutant. The values are means ± SD ($n = 4$, each n consists of 8 cells measured as a group). **F)** Map-based cloning of *QSpl-5A*. The *QSpl-5A* locus was mapped between the markers *Xbarc319* and *Xgwm595* on chromosome 5AL. It was then fine mapped to a 1.41 Mb interval flanked by markers *SNP65131* and *CAPS65272* using recombinants. The number of recombinants between the molecular markers and *QSpl-5A* is indicated. Black arrows indicate the orientation and order of the annotated high-confidence genes in the mapping region. The structure of the Q gene (*TraesCS5A03G1116700*) and a partial sequence comparison between *WSB* and *mw164* are also shown. Rectangles represent exons. The red line denotes the G/A SNP, which is found in the fifth exon of Q gene. **G, H)** Comparisons of the spike length among 3 groups in the (*mw164* × *ND2419*) F_2 population (G), as well as in the (*mw164* × *WSB*) BC_2F_2 population (H). **I)** Sanger sequencing chromatograms of the T_0 mutant harboring the desired prime edits in Q gene. The protospacer-adjacent motif sequence is highlighted in blue. The desired edits are highlighted in red. **J)** Comparison of height and spikes among KN199 and *PE-Q*^{G229S} transgenic wheat. Scale bar, 10 cm (left) and 2 cm (right). **K, L)** Statistics of the height and spike length of KN199 and *PE-Q*^{G229S} transgenic wheat. The values are means ± SD ($n = 6$). **M)** Comparison of height and spikes among KN199, *pUbi:*Q and *pUbi:*Q^{G229S} transgenic wheat. Scale bar, 20 cm (left) and 2 cm (right). **N, O)** Statistics of the height and spike length of KN199, *pUbi:*Q and *pUbi:*Q^{G229S} transgenic wheat. The values are means ± SD ($n = 5$). **P)** Median longitudinal sections through the rachises and peduncles at the booting stage (W8.5-W9) in KN199, *pUbi:*Q and *pUbi:*Q^{G229S} transgenic wheat. Arrowheads indicate the proximal end of the epidermal. The red dots marks the 3rd to 5th parenchyma selected for quantification analysis. Scale bar, 200 μm. **Q)** Average cell length of peduncle and rachis in the KN199, *pUbi:*Q and *pUbi:*Q^{G229S} transgenic wheat. The values are means ± SD ($n = 4$, each n consists of 8 cells measured as a group). **R)** Comparison of height and spike length among KN199 and 5AQ-knocked out (KO-5AQ) mutant. Scale bar, 20 cm (left) and 2 cm (right). **S** to **U)** Statistics of plant height, spike length and spikelet density of KN199 and KO-5AQ mutant. The values are means ± SD ($n = 5$). In box plots, box edges depict upper and lower quartiles, whiskers denote 1.5× interquartile range, and center line indicates median. In B-C, E, K-L, and S-U, Student's t-test was performed. In G-H, N-O, and Q, 1-way ANOVA was performed. *$P < 0.05$, **$P < 0.01$; ns, not significant.

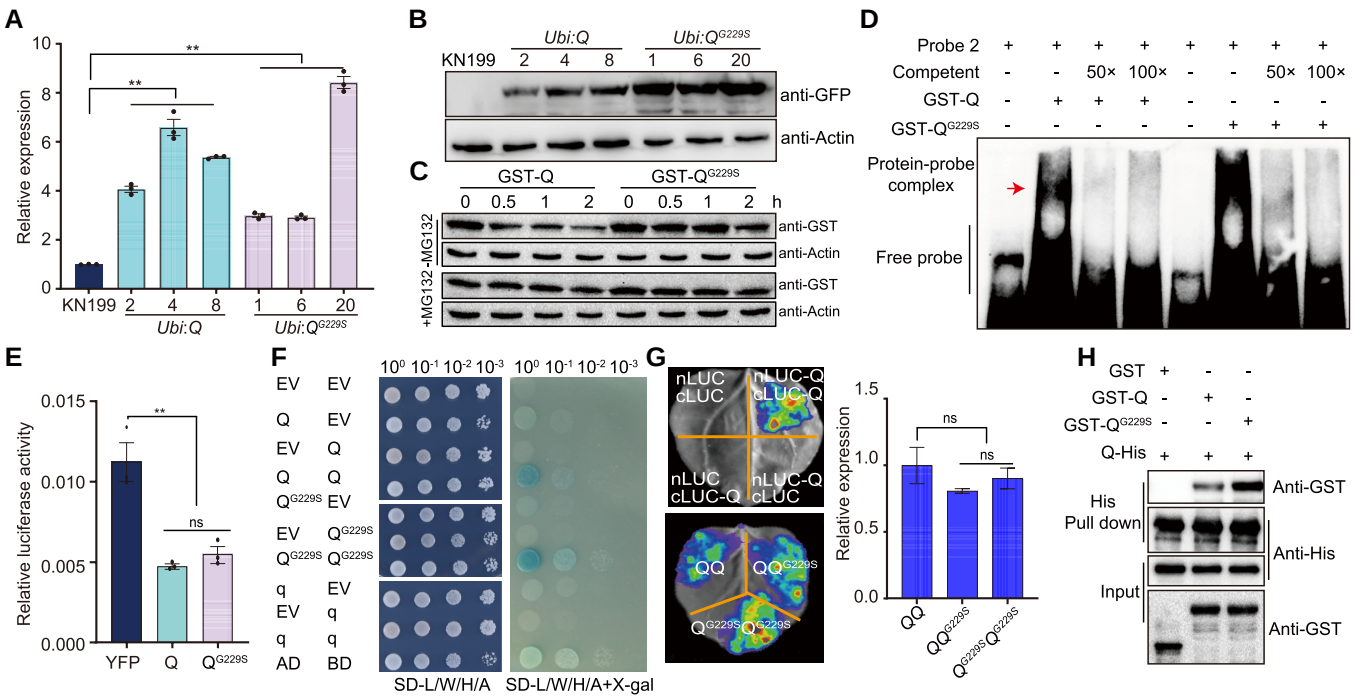

Figure 2. Q^{G229S} enhances the stability and dimer formation of Q protein. **A, B)** Transcription and protein level analyses of Q and Q^{G229S} in representative transgenic plants. 2, 4, 8 and 1, 6, 20 represent independent *pUbi*:Q and *pUbi*:Q^{G229S} lines, respectively. *GAPDH* was utilized as the internal control. The values are means ± SD ($n = 3$). **C)** Cell-free degradation assay shows that the relatively higher stability of GST-Q^{G229S} protein compared with GST-Q protein. The β-Actin in the samples indicates that roughly equal amounts of total plant extracts were used. **D)** Direct binding of Q and Q^{G229S} to the *GA3ox2* promoter in EMSAs. The biotin-labeled probes (P2) containing GCC-box motifs were derived from *GA3ox2* promoter. Competition was performed with 50-fold and 100-fold wild-type probes. The arrow represents the probe-protein complexes. **E)** The DLR assay shows that both Q and Q^{G229S} strongly suppresses the luciferase activity of GAL4-LUC. Relative luciferase activity was measured using p35S:GAL4-BD-YFP as control. The values are means ± SD ($n = 3$). (F) Y2H assays shows that the dimmer Q^{G229S} and Q^{G229S}, Q and Q, q and q. Empty vector was used as negative control. SD-L/W/H/A indicates the yeast medium without Leu, Trp, His and Ade. **G)** LCI assay for the dimmer of Q and Q^{G229S}. nLUC and cLUC empty vector was used as negative control and the quantification of Q were shown in the right. The values are means ± SD ($n = 3$). **H)** In vitro pull-down assay shows that Q-His pulls down more GST-Q^{G229S} than GST-Q (upper). The lower shows that roughly equal amounts of Q-His, GST-Q, GST-Q^{G229S} and GST (negative control) proteins were used. In A, E, and G, 1-way ANOVA was performed. $^{**}P < 0.01$; ns, not significant.

phenotypes of *pUbi*:Q^{G229S} were more severe (Fig. 1M; Supplementary Fig. S4, A to E and Table S1). Specifically, the height of *pUbi*:Q and *pUbi*:Q^{G229S} was decreased by 15.7% to 23.1% and 39.3% to 58.1%, the spike length by 20.5% to 28.6% and 38.3% to 50.7%, and spikelet density was increased by 35.8% to 45.6% and 65.7% to 74.2%, respectively (Fig. 1, N and O). Consistent results were obtained from field experiments, showing that the height of *pUbi*:Q and *pUbi*:Q^{G229S} decreased by 19.6% to 30.6% and 33.8% to 44.7%, respectively, while the spike length decreased by 33% to 41.7% and 60.4% to 64.8%. Additionally, the spikelet density increased by 62.8% to 81.3% and 135% to 158%, respectively (Supplementary Fig. S4, C to F). Similarly, the length of peduncle cells reduced by 18.7% and 35.3% and the length of rachis cells reduced by 23.5% and 47.0% in *pUbi*:Q and *pUbi*:Q^{G229S} plants, respectively (Fig. 1, P and Q). To accurately verify the function of Q, we generated 5AQ-knocked out mutants (*KO*-5AQ) by performing CRISPR/Cas9-mediated gene editing in KN199. The phenotypic analysis revealed that *KO*-5AQ mutants exhibited increased height and spike length compared with KN199; however, the spikelet density was reduced (Fig. 1, R to U; Supplementary Fig. S4, G and H and Table S1). This confirms that the point mutation (G to A) in the fifth exon of the Q gene is indeed responsible for the reducing height and spike length by enhancing Q's function.

Notably, although Q expression in the *pUbi*:Q^{G229S} lines was lower than in the *pUbi*:Q lines (Fig. 2A), the accumulation of Q^{G229S} protein remained significantly higher (Fig. 2B), suggesting enhanced stabilities of Q^{G229S}. Consequently, we evaluated the stabilities of both Q and Q^{G229S} through cell-free degradation assays. The GST-Q proteins gradually degraded in KN199 protein extracts with increasing incubation time, while the degradation of GST-Q^{G229S} proteins was moderately slower (Fig. 2C). The degradation of GST-Q was effectively blocked by the 26S proteasome inhibitor MG132 (Fig. 2C). Previous studies have reported Q as a transcriptional repressor (Liu et al. 2018). Q contains conserved AP2 domains that recognize and bind the GCC-box (AGCCGCC) and GCC-like box (xCCxCC) (Cheng et al. 2018; Yang et al. 2024). To investigate whether the G229S mutation also affect the DNA binding and transcriptional regulatory activities, we performed an electrophoretic mobility shift assay (EMSA) and a dual-luciferase reporter (DLR) assay. The results of the DLR and EMSA experiments indicate that the transcriptional activity and DNA binding activity of Q^{G229S} were not likely affected (Fig. 2, D and E).

Consistent with previous studies demonstrating the ability of Q to form homodimers (Simons et al. 2006; He et al. 2021), our yeast two-hybrid (Y2H) and luciferase complementation imaging (LCI) assays confirmed these findings. Through LCI and Y2H experiments, we found that the dimers formed by Q^{G229S} and Q^{G229S}, Q and Q^{G229S}, Q and Q, and q and q gradually decreased (Fig. 2, F and G), suggesting the G229S mutation could enhance the formation of homodimers. Furthermore, by performing immunoprecipitation with anti-His antibodies on His-Q/GST-Q^{G229S} and His-Q/GST-Q complexes, we observed that the Q^{G229S} protein was more effectively pulled down compared with the Q protein (Fig. 2H), indicating an enhancement in the formation of homodimers or heterodimers.

Because the G229S mutation is located within the AP2-R2 domain, we aimed to identify the domains responsible for the interaction by dividing the Q protein into 3 segments based on the distribution of conserved domains (Supplementary Fig. S5A). Q-middle, which contains the AP2 domain, showed strongest dimerization capability, followed with Q-C-terminal, which contains the second ethylene-responsive element binding factor-associated amphiphilic repression (EAR2) domain. However, Q-N-terminal, which contains the first EAR1 domain, did not show any dimerization ability (Supplementary Fig. S5B). Collectively, these results indicated that the G229S mutation could enhanced protein stability and homodimerization, while may bring in limited effects on DNA binding and transcriptional activities.

Q repressed GA biosynthesis through directly targeting *GA3ox2*

In wheat, although the *Rht-D1b* and *Rht-B1b* alleles (Flintham et al. 1997), as well as the overexpression of *Rht1*, do not affect spike length, knockout of *Rht-B1b* gene can increase spike length (Song et al. 2023; Xu et al. 2023). The overexpression lines of *Q*/Q^{G229S} exhibit typical GA-deficient phenotypes, including dwarfism and shortened spikes (Fig. 1J; Supplementary Fig. S4, A to E), while the relationship between Q and GA is still not clear. Therefore, we investigated the effects of exogenous application of GA_3 on phenotypic changes of *Q*/Q^{G229S} overexpression plants. In the greenhouse, 50 μM GA_3 was sprayed on the leaves of KN199, *pUbi*:Q and *pUbi*:Q^{G229S} wheat from vernalization until heading. We discovered that the application of GA_3 could partially restore both the height and spike length deficiencies of *Q*/Q^{G229S} overexpression lines (Fig. 3, A and B; Supplementary Fig. S6, A and B). Specifically, there was an increase of 8.9% in height and 9.3% in spike length for KN199. The height and spike length of the *pUbi*:Q lines were restored to 99.0% and 98.4 of the untreated KN199, while the height of the *pUbi*:Q^{G229S} lines also reached 85.4% and 74.8% of the untreated KN199. Furthermore, GA_3 treatment of the *pUbi*:Q^{G229S} lines resulted in the restoration of height and spike length to levels comparable to those observed in untreated *pUbi*:Q lines (Fig. 3C). Additionally, the spikelet densities were decreased by 17.7% and 22.8% in Q and Q^{G229S} overexpression lines, respectively (Fig. 3D). Moreover, the content of GA_1, GA_4 (synthesized by *TaGA3ox2*) was significantly decreased in spikes (W3.5 stage) and peduncles of *Q*/Q^{G229S} overexpression lines (Fig. 3E), as well as in the *wm164* mutant (Supplementary Fig. S6C). These results suggest that the semi-dwarf phenotypes in *Q*/Q^{G229S} overexpression lines were partially attributed to the deficiency of GA biosynthesis.

We subsequently examined the transcription levels of GA synthesis genes, including *GA3ox2*, *TaKS1*, *TaKO2*, *TaGA20ox1*, *TaGA20ox2*, *TaGA20ox3*, in spikelets, rachises and peduncles of *Q*/Q^{G229S} overexpression lines (Supplementary Fig. S6, D to F). Only the transcription levels of *GA3ox2* showed significant decrease in all the 3 tissues of *Q*/Q^{G229S} overexpression lines compared with KN199 (Fig. 3F), as well as in the *wm164* mutant (Supplementary Fig. S6G). Meanwhile, we found that the expression level of *GA3ox2* was significantly elevated in *KO*-5AQ (Supplementary Fig. S6H). The expression of the *KS1* gene was upregulated in the rachises and peduncles of both *Q*/Q^{G229S} overexpression lines compared with KN199; however, the other 5 genes showed downregulation specifically in the rachis (Supplementary Fig. S6, D to F). Through RNA-seq analysis, we found no difference in the expression levels of the *GA2-oxidase* gene *TraesCS6A02G221900* (*TaGA2ox-A9*), *TraesCS6B02G259200* (*TaGA2ox-B9*), *TraesCS6D02G213100* (*TaGA2ox-D9*) in the young spikes of WSB and *mw164*. In contrast, the expression levels of these genes were slightly elevated in the young spikes of *pUbi*:Q compared with those of KN199 and *KO*-5AQ. However, there was no difference in the expression of the *GA2-oxidase* genes *TraesCS3A02G537300* (*TaGA2ox-A11*), *TraesCS3B02G603000* (*TaGA2ox-B11*), and *TraesCS3D02G542800* (*TaGA2ox-D11*) between the young spikes of KN199 and *KO*-5AQ (Supplementary Fig. S6I).

We then analyzed the TFs binding motifs within the promoter region of *GA3ox2*, which identified 4, 6, and 8 Q binding motif CCGNC in the *GA3ox2* promoter regions in A, B, and D subgenomes, respectively (Fig. 3G). The binding between Q proteins and those motifs were validated by EMSA experiments except P5 (Fig. 3H). Through dual-luciferase systems, we found that both Q and Q^{G229S} could repress the expression of the reporter gene. It was worth noting that Q and Q^{G229S} exhibit a stronger repression effect on the *GA3ox2-D1* promoter, a moderate effect on the *GA3ox2-B1* promoter, and a weaker effect on the *GA3ox2-A1* promoter (Fig. 3I), indicating regulatory differentiations among the subgenomes. To further investigate the in vivo binding, we conducted chromatin immunoprecipitation (ChIP) assays with anti-GFP beads, and confirmed that the P1, P2, P3, and P5 regions of the *GA3ox2* promoter were significantly enriched in both *Q*/Q^{G229S}-*GFP* overexpression lines (Fig. 3J).

To further validate that *GA3ox2* is indeed a target gene of Q, we generated *pUbi*:*GA3ox2* transgenic wheat in KN199, utilizing the complete coding sequence (CDS) of *GA3ox2* driven by *Ubiquitin* promoter. Compared with KN199, the height and spike length of *pUbi*:*GA3ox2* lines were not significantly different (Supplementary Fig. S6, J to M). However, overexpression of *GA3ox2* similarly rescued both traits: in the *pUbi*:Q line, height and spike length were restored to 92.2% and 70.3% of KN199, and in the *pUbi*:Q^{G229S} line, to 74.9% and 59.4%, respectively (Fig. 3, K to M; Supplementary Table S1). These results align with the trend observed under GA_3 treatment and revealed that Q inhibited GA biosynthesis via directly repressing the expression of *GA3ox2*.

Stabilization of RHT1 enhanced through competitive interaction between Q and *Ta*GID2

Considering that the exogenous application of GA_3 and the overexpression of *GA3ox2* do not fully restore the semi-dwarf and compact spike phenotypes of *Q*/Q^{G229S} overexpression lines (Fig. 3, A and B), we speculated that Q may also be involved in GA signaling pathways in wheat. We found that the abundances of both Q and Q^{G229S} proteins remained unchanged after treatment with 50 μM GA_3 (Supplementary Fig. S7A).

Therefore, we further investigated the interaction between Q and RHT1, *Ta*GID1 and *Ta*GID2. Y2H assays showed that Q could directly interact with RHT1 and GID2, but not GID1 (Fig. 4A; Supplementary Fig. S7B), which was further confirmed by LCI assays and bimolecular fluorescence complementation (BiFC) assays (Fig. 4, B and C). We also performed the Co-Immunoprecipitation (Co-IP) assays and revealed that Q and Q^{G229S} could physically interact with RHT1 in vivo (Fig. 4D). In addition, we observed a strong interaction between Q and RHT1-C-terminal, which contains the GRAS domain, while no interactions were detected between Q and RHT1-N-terminal, which contains the DELLA domain and poly S/T/V domain (Supplementary Fig. S7, C and D). We investigated the expression of *Q*, *Rht-1*, and *GID2* through WheatOmics and found that these genes are expressed in the peduncle, spike and spikelet tissue

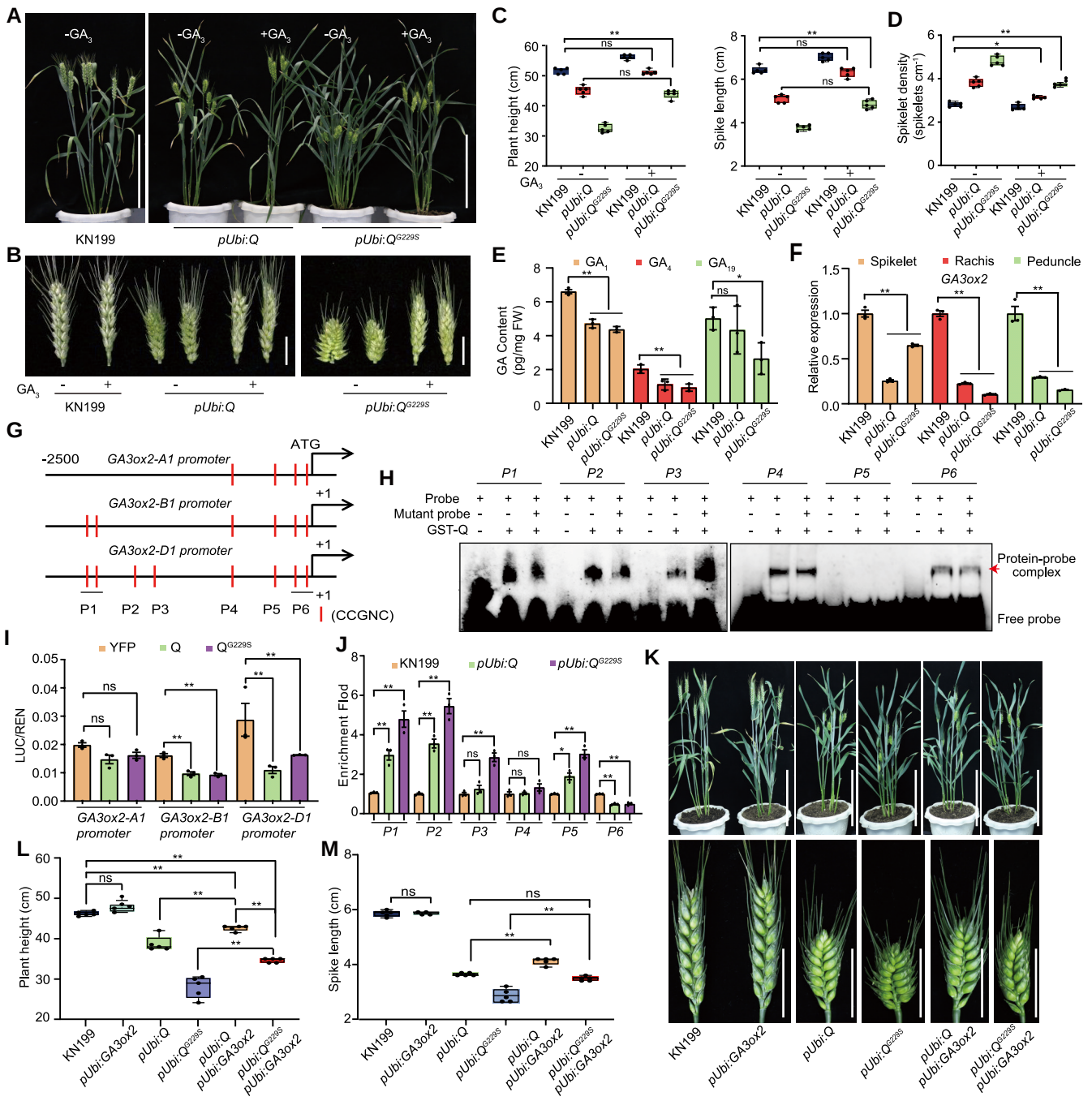

Figure 3. Q represses the transcription of *GA3ox2* and negatively regulate GAs biosynthesis in wheat. **A, B)** The height and spike length of KN199, *pUbi*:Q and *pUbi*:Q^{G229S} transgenic wheat treated with or without 50 μM GA_3. Scale bars, 20 cm for the whole-plant images (A) and 2 cm for spike images (B). **C-D)** Statistical analysis of the height, spike length and spikelet density in KN199, *pUbi*:Q and *pUbi*:Q^{G229S} transgenic wheat treated with or without 50 μM GA_3. The values are means ± SD ($n = 5$). **E)** Measurement of GA content in mixed samples of spikes and peduncles (stage W3.5) from KN199, *pUbi*:Q and *pUbi*:Q^{G229S} transgenic wheat. Error bars indicate ± SD ($n = 3$). FW, fresh weight of mixed spike and peduncle. **F)** qRT-PCR results showing the expression levels of *GA3ox2* genes in spikelet, rachis and peduncle of KN199, *pUbi*:Q and *pUbi*:Q^{G229S} transgenic wheat. *GAPDH* was used as the internal controls. The values are means ± SD ($n = 3$). **G)** The schematic representation of different regions, which include the AP2 binding element (CCGNC) in the promoter of *GA3ox2-A1/B1/D1*. **H)** Direct binding of Q to the *GA3ox2* promoter in EMSAs. The biotin-labeled probes (P1-P6), containing GCC-box motifs, were derived from the *GA3ox2* promoter, while the mutant probes, in which the GCC-box was replaced with (AAAAAA). **I)** Transient dual LUC reporter assays showing that Q and Q^{G229S} repressed transcription of *GA3ox2-A1/B1/D1*. YFP was used as a control. The values are means ± SD ($n = 3$). **J)** ChIP-PCR assay showing enrichment of the promoter fragments of *GA3ox2pro* bound by Q and Q^{G229S} in *pUbi*:Q and *pUbi*:Q^{G229S} transgenic wheat. Anti-GFP antibodies were used for precipitation. KN199 with anti-GFP antibodies were used as negative controls. The values are means ± SD ($n = 3$). **K)** The height and spike length of the KN199, *pUbi*:*GA3ox2*, *pUbi*:Q/*pUbi*:*GA3ox2*, *pUbi*:Q^{G229S}/*pUbi*:*GA3ox2*, *pUbi*:Q and *pUbi*:Q^{G229S}. Scale bar, 20 cm (up) and 3 cm (bottom). **L** to **M)** Statistical analysis of the height and spike length of KN199, *pUbi*:*GA3ox2*, *pUbi*:Q/*pUbi*:*GA3ox2*, *pUbi*:Q^{G229S}/*pUbi*:*GA3ox2*, *pUbi*:Q and *pUbi*:Q^{G229S}. The values are means ± SD ($n = 5$). In box plots, box edges depict upper and lower quartiles, whiskers denote 1.5× interquartile range, and center line indicates median. In E-F, and I-J, 1-way ANOVA was performed. In C-D, L-M, 2-way ANOVA was performed. $^{*}P < 0.05$, $^{**}P < 0.01$; ns, not significant.

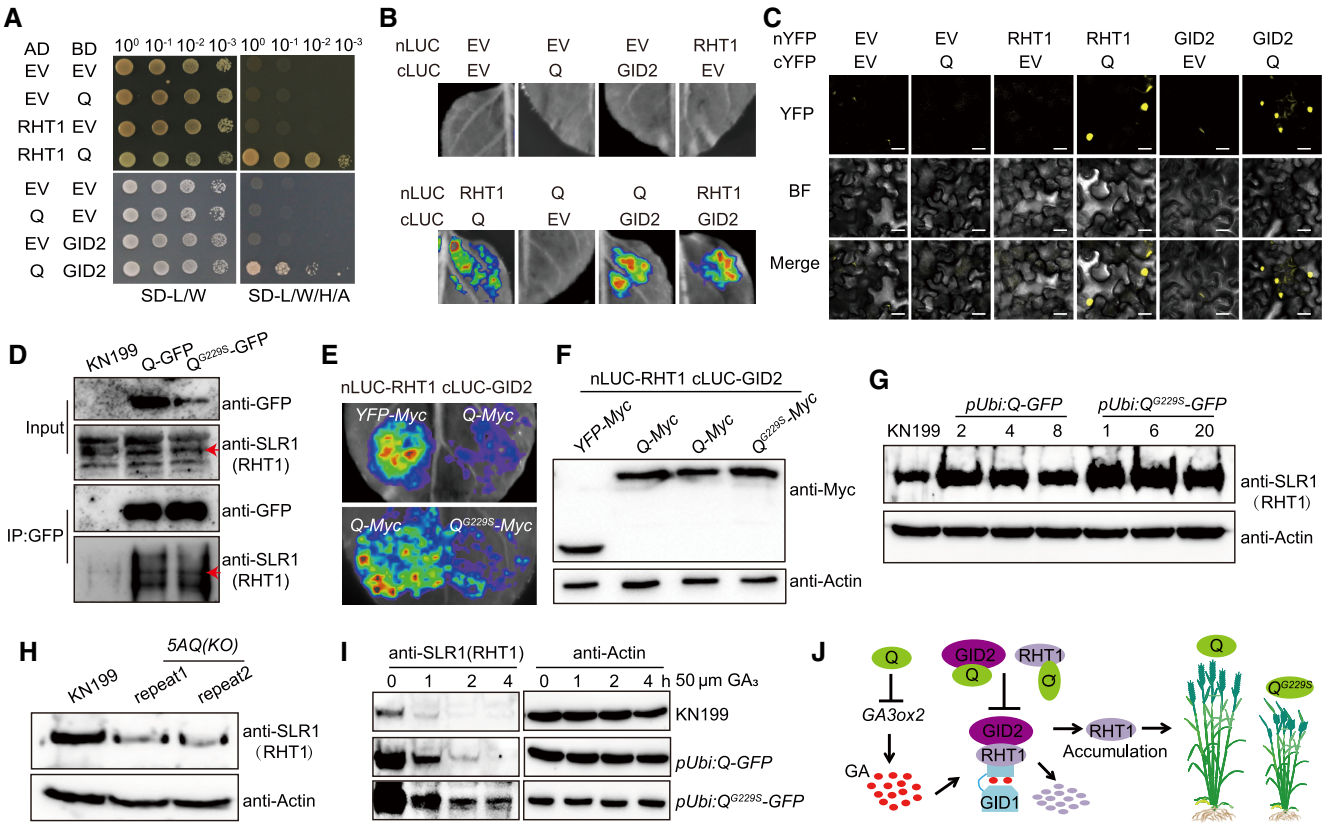

Figure 4. Q blocks the GA signaling by interacting with RHT1 and GID2 to antagonize the GID2-triggered degradation of RHT1. **A)** Y2H assay shows that Q interacts with RHT1 and GID2. SD-L/W, indicates the yeast medium without Leu and Trp; SD-L/W/H/A indicates the yeast medium without Leu, Trp, His, and Ade. **B)** LCI assay shows Q, RHT1 and GID2 interact with each other in *N. benthamiana*. **C)** BiFC analysis shows that Q interacts with RHT1 and GID2 in *N. benthamiana*. YFP, eYFP fluorescence; BF, bright-field image. Scale bar, 20 μm. **D)** Co-IP assays for the interactions between Q and RHT1 in wheat. Total protein was extracted from KN199, *pUbi*:Q and *pUbi*:Q^{G229S} transgenic wheat and immune precipitated by Anti-GFP Magnetic Beads. anti-GFP and anti-SLR1 antibodies were used for immunoblots. The arrow indicates RHT1 (SLR1). **E)** LCI assays show that Q and Q^{G229S} inhibit the interaction between RHT1 and TaGID2 in *N. benthamiana*. YFP-Myc was used as a control. **F)** Western blotting analysis shows the presence of YFP-Myc, Q-Myc and Q^{G229S}-Myc in the infiltrated areas of *N. benthamiana* leaves. **G, H)** Accumulation of RHT1 (Anti-SLR1) in *pUbi*:Q, *pUbi*:Q^{G229S} and KO-5AQ transgenic wheat. 2, 4, 8 and 1, 6, 20 represent independent *pUbi*:Q, *pUbi*:Q^{G229S} lines, respectively. **I)** Time-course analysis of RHT1 degradation in KN199, *pUbi*:Q and *pUbi*:Q^{G229S} transgenic wheat treated with 50 μM GA_3. The β-Actin levels in the samples indicate that approximately equal amounts of total plant extracts were used. **J)** A model illustrating the dual suppressive roles of Q in both the biosynthesis and signaling pathways of GAs, leading to a reduction in height and spike length in wheat. GA (gibberellin), Q, RHT1 (reduced height1), GID1 (gibberellin insensitive dwarf1) and GID2 is represented by red, green, light purple light blue, and purple ovals, respectively. "→" and "⊥" indicates promotion and inhibition, respectively.

(Supplementary Fig. S7E) (data from International Wheat Genome Sequencing Consortium (IWGSC) 2018). Given the interactions among Q, RHT1, and GID2, we hypothesized that Q might disrupt the interaction between RHT1 and GID2. As expected, both Q and Q^{G229S} significantly inhibited the interaction between RHT1 and GID2 compared with YFP-Myc, with Q^{G229S} displaying an even more pronounced inhibitory effect (Fig. 4, E and F). Subsequently, we evaluated the protein levels of RHT1 and observed that the Q/Q^{G229S} overexpression lines and the *wm164* mutant exhibited higher accumulation of endogenous RHT1 protein compared with KN199 and WSB, particularly in the *pUbi*:Q^{G229S} lines (Fig. 4G; Supplementary Fig. S7F). In contrast, the accumulation of RHT1 in *KO-5AQ* mutants was significantly reduced compared with KN199 (Fig. 4H). Upon treatment with 50 μM GA_3, the amount of endogenous RHT1 protein was markedly reduced in KN199, *pUbi*:Q and *pUbi*:Q^{G229S} while more residual RHT1 protein remained in *pUbi*:Q^{G229S} lines (Fig. 4I), suggesting that Q could suppress the degradation of RHT1.

To further elucidate the role of Q in GA signaling pathways, we conducted experiments using KN199, *pUbi*:Q, and *pUbi*:Q^{G229S} lines under 50 μM paclobutrazol (PAC) treatment and varying concentrations of GA_3. Treatment with 50 μM PAC resulted in a reduction in height by 10.2%, 9.6%, and 2.1% in KN199, *pUbi*:Q, and *pUbi*:Q^{G229S}, respectively, while spike length decreased by 14.5%, 10.2%, and 5.3% (Supplementary Fig. S8). Upon application of 50 μM and 100 μM GA_3, KN199 displayed the greatest height and spike length, followed by *pUbi*:Q, with *pUbi*:Q^{G229S} exhibiting the smallest values. Compared with KN199 treated with PAC, treatment with 50 μM and 100 μM GA_3 resulted in height recoveries of 17.9% and 19.0% for KN199, −3.2% and −2.3% for *pUbi*:Q, and −12.6% and −11.8% for *pUbi*:Q^{G229S}, respectively. For spike length, the recoveries were 29.6% and 31.2% for KN199, 2.8% for both *pUbi*:Q treatments, and −11.1% and −11.4% for *pUbi*:Q (Supplementary Fig. S8). These results indicate that Q, particularly the Q^{G229S} allele, exhibited a reduced response to GA_3, as evidenced by a descending gradient of phenotypic recovery: KN199 > *pUbi*:Q > *pUbi*:Q^{G229S} (Supplementary Fig. S8), which also suggests that Q may play an important role in GA signaling pathways.

Discussion

Q was initially identified as a domestication gene as its mutation could alter the free-threshing characteristic, which facilitates wheat harvesting (Simons et al. 2006). Besides the roles in seed

shattering, Q also exhibits pleiotropic effects on development, including the regulation of height, spike length, and heading date. However, the mechanisms by which Q regulates these agronomic traits is still elusive. Here, we identified an allele Q^{G229S} and proposed a molecular model of Q negative regulation of GAs synthesis and signaling pathway (Fig. 4J). The G to A substitution in the fifth exon of Q did not alter its expression (Supplementary Fig. S3C), but it enhanced its protein stability and homodimerization ability (Fig. 2), resulting in semi-dwarf and compact spike. Notably, the G229S mutation is located adjacent to the conserved WEAR motif in the YRG element, which is crucial for DNA binding (Okamuro et al. 1997). Nevertheless, the EMSA and LUC reporter assays revealed no significant difference between Q and Q^{G229S} regarding their DNA binding affinity and transcriptional regulatory activity (Fig. 2, D and E). Hence, it remains unclear whether the G229S mutation affects the phosphorylation modification of the Q protein, and subsequently influences its function.

Our study reveals that Q diminishes GA content in both spikes and peduncles by inhibiting the expression of *GA3ox2* (Fig. 3; Supplementary Fig. S6). Several studies have reported that AP2/ERF TF, such as *Os*RPH1 and *Os*AP2-39 could repress endogenous GA levels, leading to decreased height, internode length, and leaf sheath length in rice (Yaish et al. 2010; Ma et al. 2020). Additionally, the application of GA_3 has been demonstrated to partially reverse the miR172-mediated suppression of *HvAP2*, leading to shorter stems in barley (Patil et al. 2019), which suggests a conserved relationship between AP2 TFs and GA synthesis among various plant species.

The height of *pUbi*:Q and *pUbi*:Q^{G229S} lines was reduced to approximately 76.9% to 84.3% and 41.9% to 60.7% of KN199, respectively. Since GA_3 treatment or *GA3ox2* overexpression can compensate for deficiencies in GA biosynthesis, we used the degree of phenotypic restoration toward the untreated KN199 as a proxy for GA responsiveness. Upon GA_3 treatment, their heights partially recovered to 99.0% and 85.4% of untreated KN199 (Fig. 3, A to C), while spike length increased from 71.4%–79.5% and 49.3%–61.7% to 98.4% and 74.8%, respectively. Overexpression of *GA3ox2* similarly rescued both traits: in *pUbi*:Q, height and spike length were restored to 92.2% and 70.3% of KN199, and in *pUbi*:Q^{G229S} to 74.9% and 59.4%, respectively (Fig. 3, K to M). Additionally, in the GA_3 and PAC co-treatment experiment, a descending trend of phenotypic recovery was observed across genotypes: KN199 > *pUbi*:Q > *pUbi*:Q^{G229S} (Supplementary Fig. S8).

These results demonstrate that both Q alleles retain partial responsiveness to GA_3, but their response to GA_3 treatment is significantly reduced compared with KN199. Notably, *pUbi*:Q^{G229S} exhibited the weakest recovery under both GA_3 treatment and *GA3ox2* overexpression, suggesting that the G229S mutation exacerbates the reduced GA responsiveness. This trend was also confirmed by the 2-way ANOVA showing a significant genotype-by-treatment interaction. Therefore, we conclude that Q, particularly the Q^{G229S} allele, confers reduced responsiveness to GA_3 treatment. However, it remains possible that the increased RHT1 protein accumulation observed in these lines is an indirect result of altered endogenous GA levels rather than a direct consequence of Q-GID2-RHT1 interaction (Fig. 4, G to I), a hypothesis that warrants further investigation.

Q enhances free-threshing characteristics and reduces height, which aids in refining wheat architecture. However, an overabundance of the Q protein can lead to undesirable outcomes such as dwarfism and compact spikes, negatively impacting wheat yield. Further investigation into whether these 2 traits operate independently and how to adjust the Q-related pathways to control height and spike length individually could significantly advance the utilization of diverse Q alleles. In summary, our study has not only deepened our understanding of how Q regulates height and spike length but also established a connection between this crucial domestication gene and GA pathways.

Materials and methods

The elite spring wheat variety Nanda 2419 (ND2419), systematically selected and bred from the Italian accession *Mentana*, and the Chinese wheat landrace WSB, was used as a parental line for crossing with the *mw164* mutant. Fine-scale mapping of *mw164* was performed based on 2 populations: the F_2 population of *mw164*×ND2419 and BC_2F_2 population of *mw164*×WSB. Genomic DNA sequences in the candidate region were compared between *mw164* and WSB. Primer sequences used for map-based cloning in Supplementary Data Set 1 and genotyping assays were provided in Supplementary Tables S2 and S4.

Re-sequencing and SNP calling

The genomic DNA of WSB and *wm164* was extracted using a standard CTAB method (Huang et al. 2000), and 1 μg DNA per sample was fragmented by sonication to an average size of 300–400 bp. The libraries containing selected fragments were sequenced using a BGISEQ-500 platform with a paired-end read length of 150 bp. We filtered the raw data using SOAPnuke (Chen et al. 2018) and obtained clean reads with a sequencing depth of 12-fold coverage.

The remaining high-quality reads were mapped to CS reference genome v2.1 (Zhu et al. 2021) using the Burrows-Wheeler Alignment tool (BWA, Li and Durbin 2009). The duplicated reads were marked and removed using the Genome Analysis Toolkit (GATK, McKenna et al. 2010). The GATK HaplotypeCaller module was used to identify the SNPs between WSB and *wm164*. The genic positions (e.g. intragenic, upstream, downstream, and intergenic) and associated functions of all variants were further annotated using ANNOVAR software (Wang et al. 2010) based on the CS reference genome v2.1.

Transgene constructs

The CDS of Q, Q^{G229S} and *TaGA3ox2* were amplified and inserted into the *110-pUbi:GFP* and *110-pUbi:Myc* vector, which are derived from the PWMB111 vector backbone (Wang et al. 2022). Then the PCR product and 110-pUbi vector were ligated to generate *pUbi:Q-GFP*, *pUbi:*Q^{G229S}*-GFP* and *pUbi:GA3ox2-Myc* constructs. For CRISPR/Cas9-based gene editing, sgRNA target sequences were designed according to the exon sequences of 5AQ. The MT_1T_2 vector was amplified by 1 pair of primers containing the sgRNAs and then cloned into the CRISPR/Cas9 vector pBUE413 (Xing et al. 2014). We designed pegRNA sequences using PlantpegDesigner (Lin et al. 2021). The pUC57-CmYLCV vector was amplified by pegRNA primer, pegRNA sequence (contain the CmYLCV promoter and CaMV terminator) was cloned into the pUC57-CmYLCV vector (Ni et al. 2023). The recombinant plasmids were transfected into *A. tumefaciens* strain EHA105. The transgenic wheat was generated by *Agrobacterium*-mediated transformation into 15-d-old immature embryos of KN199 (Ishida et al. 2015). Relevant primer sequences are given in Supplementary Data Set 1.

Growth conditions and GA_3 treatment

The F_2 and BC_2F_2 populations in this study were planted in a 2.0 m single-row plot spaced 0.3 m apart with 20 seeds per

row at Chinese Academy of Agricultural Sciences-Xinxiang Experimental Station (Qiliying county, Xinxiang city, Henan province) in the 2020 to 2021 natural growing season. The T_2 of Q and Q^{G229S} overexpression lines were planted in a 1.0 m single-row plot spaced 0.3 m apart with 10 seeds per row at Chinese Academy of Agricultural Sciences Experimental Station (Beijing, People's Republic of China) in the 2021 to 2022 natural growing season. The agronomic traits including height, spike length, spikelet numbers per spike were measured manually before harvest in the field. For qRT-PCR assays, phytohormone treatments, Co-IP assays and ChIP-PCR assays, the plants of KN199, Q and Q^{G229S} overexpression wheat were grown in a greenhouse under 16 h of light at 24 °C and 8 h of dark at 19 °C.

GA_3 (A600738, Sangon Biotech) was dissolved in dimethyl sulfoxide (DMSO). KN199, Q and Q^{G229S} overexpressing lines were transplanted to a greenhouse with conditions of 16 h of light at 24 °C and 8 h of dark at 19 °C after vernalization. Every day after dark, 5 mL of 50 μM GA_3 was sprayed onto the leaves of KN199, Q and Q^{G229S} overexpressing plants until heading. An equal volume of DMSO was used as a mock control. Height and spike length were measured at the heading stage. All experiments were performed in 3 biological replicates.

Histological observations

The rachises and peduncles at the booting stage (W8.5-W9) of WSB, *mw164*, KN199, Q and Q^{G229S} overexpression wheat lines were fixed in FAA solution, embedded in paraffin, longitudinally sectioned, stained with 0.1% Toluidine blue O, and observed using a Axio Imager Z2 (Carl Zeiss). Cell lengths of each sample were measured on 3 serial sections of the rachis and peduncle.

qRT-PCR analysis and RNA-seq assays

Total RNAs were extracted from leaves, spikelets, rachises, peduncles at the booting stage (W5-W6) of WSB, *mw164*, KN199, Q and Q^{G229S} overexpression wheat using the TRIzol reagent (Invitrogen, 15596–026), the full-length cDNAs were reverse-transcribed using FastKing RT Kit (TIANGEN; KR116), according to the manufacturer's protocol. Subsequent qRT-PCR was performed using TB Green Premix Ex TaqII (TaKaRa) and LightCycler96 (Roche), with each qRT-PCR assay being replicated at least 3 times with 3 independent RNA preparations. *TaGAPDH* gene transcript was used as the internal control. Relevant primer sequences are given in Supplementary Data Set 1.

For RNA-sequencing analysis, the young spikes (W3.5) of WSB, *mw164*, KN199, *pUbi:Q*, and *KO-5AQ* samples were collected at W3.5 stage, and total RNAs were extracted using TRIzol Reagent. The RNA-Seq library was constructed by Berry Genomics (Beijing, China), and sequenced with Illumina NovaSeq 6000 platform. All sequencing data were 150 bp paired-end reads. For data quality control, we used fastp v0.21.0, and reads were aligned to CS reference genome v1.0 using hisat2 (https://daehwankimlab.github.io/hisat2/) with default parameters. BAM files were sorted using SAMtools v1.3.1, read counts was quantified using FeatureCounts, and Transcripts Per Million values were calculated using TPMCalculator. The RNA-seq data generated in the current study are available in the Gene Expression Omnibus database (https://www.ncbi.nlm.nih.gov/geo) under accession number GSE298823.

Luciferase transient transcriptional repression assay

The GAL4 reporter plasmid contains the Firefly luciferase (LUC) gene fused with GAL4 binding site, the *p35S:REN* (the Renilla luciferase) reporter plasmid as the internal control. The CDS of Q, Q^{G229S} and *YFP* were amplified and fused into the *p35S:GAL4-BD* vector to construct the effecter plasmids, respectively. The effector and reporter plasmids were co-transformed in *N. benthamiana* protoplasts, and the *p35S:GAL4-BD-YFP* vector was used as a control. The DLR assay system (Promega, E1910) was used to measure firefly LUC and REN activities. For each transformation, 10 μg of reporter plasmid and 10 μg of effector plasmid were used. Relative REN activity was used as an internal control, and LUC/REN ratios were calculated. At least 3 measurements were performed for each assay. Relevant primer sequences are given in Supplementary Data Set 1.

Western blotting assays

Total proteins were extracted using 2× Laemmli buffer (125 mM Tris-HCl pH 6.8, 4% SDS, 20% glycerol, 0.001% Bromophenol blue) (Laemmli 1970), and electrophoretically separated by 8% or 10% SDS-PAGE and transferred to Amersham Protran NC (GE, 10600002). Proteins were detected by immunoblot using the antibodies: anti-SLR1 (1:2000, ABclonal, A16279), anti-GFP (1:2000, Roche, 11814460001), anti-Myc (1:5000, Roche, 11667149001), β-Actin (1:5000, CWBIO, CW0264 M), anti-GST (1:3000, CWBIO, CW0084), and anti-His (1:3000, CWBIO, CW0286), anti-mouse IgG (1:75000, Sigma, A9044-2ML), anti-Rabbit IgG (1:5000, phytoab, PHY6000), respectively.

In vitro pull-down

The CDS of Q and Q^{G229S} was amplified and inserted into the pGEX4T-1 or pET28a vector. The recombinant GST-Q, GST-Q^{G229S} and His-Q protein were expressed in *Escherichia coli* BL21 (DE3) (Transgen, CD701-01), and then purified and immobilized on BeaverBeads GSH (Beaver, 70601-5) and BeaverBeads IDA-Nickel (Beaver, 70501-5) following the manufacturer's instructions. Equal amounts of eluted GST-Q, GST-Q^{G229S} and His-Q proteins were incubated with BeaverBeads IDA-Nickel in the column buffer (20 mM Tris-HCl pH 8.0, 200 mM NaCl, 1 mM EDTA, 10 mM PMSF) at 4 °C for 2 h. Then, the beads were washed 5 times with washing buffer (20 mM Tris-HCl pH 8.0, 200 mM NaCl, 1 mM EDTA), followed boiling with 2× Laemmli buffer. Supernatants were electrophoretically separated by 10% SDS-PAGE and subjected to immunoblotting using anti-GST, and anti-His, anti-mouse IgG antibodies. Relevant primer sequences were given in Supplementary Data Set 1.

Cell-free protein degradation assays

Three-week-old seedlings of KN199 were harvested. The total proteins were extracted with lysis buffer [50 mM Tris-HCl pH 8.0, 50 mM MES, 1 mM $MgCl_2$, 10 mM EDTA, 5 mM DTT, 10 mM PMSF, 1× proteinase inhibitor cocktail (Roche, 04693132001) and 10 μM ATP (Invitrogen, 18330019)]. For the degradation assays, the purified GST-Q and GST-Q^{G229S} (about 500 ng) were incubated in 50 μL of wheat total protein extract (containing about 200 μg total proteins). The samples were harvested from the mixtures for a series of incubation times at 28 °C, and processed for western blot analysis to determine the abundances of GST-Q, GST-Q^{G229S}. Western blotting was performed using anti-GST, anti-β-Actin and anti-mouse IgG antibodies. The β-Actin in the samples indicating the roughly equal amounts of total plant extracts were used.

Y2H assays

The CDS of Q, Q^{G229S}, *q*, *Rht1*, *GID1*, *GID2*, and truncated Q were amplified and cloned into pGBKT7 (Baits) or pGADT7 (Preys),

respectively. The different combinations of prey and baits were co-transformed into yeast strain AH109. Positive clones were transferred to SD-Trp/Leu and SD-Trp/Leu/His/Ade on solid medium to detect the interactions. The combinations of prey and pGBKT7 were used as the negative control. Relevant primer sequences were given in Supplementary Data Set 1.

LCI assays

The LCI assays were performed in *N. benthamiana* leaves. The CDS of Q, Q^{G229S}, *Rht1*, and *GID2* were amplified and cloned into *pCAMBIA1300-35S:nLUC* or *pCAMBIA1300-35S:cLUC* vectors to generate fusion constructs, respectively (Chen et al. 2008). The recombinant plasmids were transformed into *A. tumefaciens* strain GV3101 separately, and then combinations and the *p19* co-infected into *N. benthamiana* leaves. The injected leaves were sprayed with 1 mM luciferin (Promega, E1601) and the LUC signals were captured 48 h later using a cooled CCD imaging apparatus (Berthold, LB985). The assay was repeated at least 3 times and 8 independent leaves were used for each experiment. Relevant primer sequences were given in Supplementary Data Set 1.

EMSA

The GST fused Q and Q^{G229S} protein were expressed in *Escherichia coli* BL21 (DE3) (Transgen, CD701-01), and then purified with BeaverBeads GSH (Beaver, 70601-5) following manufacturer's instructions. The *GA3ox2* promoter probes containing the GCC-box were labeled and 5′biotin modification was synthesized in Beijing Genomics institution. EMSAs were performed as LightShift Chemiluminescent EMSA Kit (Thermo, 20148). Each experiment was independently replicated 3 times.

BiFC assays

The CDS of Q, *Rht1* and *GID2* were amplified and cloned into *p35S:cYFP* or *p35S:nYFP* vectors (YFP, yellow fluorescent protein) to generate fusion constructs, respectively. The recombinant plasmids were transformed into *A. tumefaciens* strain GV3101 separately. Co-transfection of constructs into *N. benthamiana* leaves. The YFP signal was captured using a confocal microscope (Laser at 514 nm, laser intensity at 20%, collection bandwidth from 510 to 620 nm, gains from 900 to 1200) after 48 h (Carl Zeiss, LSM880). The assay was repeated at least 3 times and 4 independent leaves were used for each experiment. Relevant primer sequences are given in Supplementary Data Set 1.

Co-IP assays

For Co-IP experiments, total proteins were extracted from KN199, Q and Q^{G229S} overexpression wheat leaves at tillering stage with a lysis buffer (50 mM Tris-HCl PH 7.5, 150 mM NaCl, 10 mM $MgCl_2$, 5 mM EDTA, 0.1% Triton X-100, 0.2% NP-40, 10 mM PMSF, 20 μM MG132, 1× proteinase inhibitor cocktail). Lysates were incubated with magnetic beads conjugated with an anti-GFP-tag antibody (MBL, M153-10) at 4 °C for 6 h. The magnetic beads were then washed 5 times with washing buffer (50 mM Tris-HCl PH 7.5, 150 mM NaCl, 10 mM $MgCl_2$, 5 mM EDTA, 0.1% Triton X-100, 0.2% NP-40). Immunoprecipitates were electrophoretically separated and specific proteins detected by immunoblotting with anti-GFP, anti-SLR1, anti-mouse IgG, anti-Rabbit IgG antibodies, respectively.

Luciferase transient expression assay

The 2.5 kb promoter sequences of *GA3ox-A2/B2/D2* were amplified and cloned into a pGreenII-0800-LUC/REN vector, respectively (Hellens et al. 2005). For the construction of the effectors, Q, Q^{G229S}, and *YFP* were cloned into the p2GW7 vector (Niu et al. 2015). The effector and reporter plasmids were co-transformed in *N. benthamiana* protoplasts, the p2GW7-YFP vector was used as a control. The DLR assay system (Promega, E1910) was used to measure firefly luciferase and renilla luciferase activities. For each transformation, 10 μg of reporter plasmid and 3 μg of effector plasmid were used. Relative REN activity was used as an internal control, and LUC/REN ratios were calculated. At least 3 measurements were performed for each assay.

ChIP-PCR assay

ChIP assays were performed as described (Gendrel et al. 2005). Two grams of each sample of KN199, Q and Q^{G229S} overexpression wheat leaves were collected at tillering stage. Samples were immediately fixed with 1% (v/v) formaldehyde under vacuum 2 times (15 min/time) at 25 °C, then terminated by adding 0.25 M glycine under vacuum for 5 min at 25 °C. The samples were ground to powder in liquid nitrogen and suspended in extraction buffer I (50 mM HEPES pH7.5, 150 mM NaCl, 1 mM EDTA, 0.1% Triton X-100, 10% glycerol, 1× proteinase inhibitor cocktail, 5 mM β-mercaptoethanol), then mixed gently at 4 °C for 30 min. The suspension was centrifuged at 1500 × *g* at 4 °C for 20 min. The nuclei were resuspended in extraction buffer II (50 mM HEPES pH7.5, 150 mM NaCl, 1 mM EDTA, 0.1% Triton X-100, 10% glycerol, 1× proteinase inhibitor cocktail) and centrifuged at 1500 × *g* at 4 °C for 20 min, and this step was repeated 3 times. The nuclei were resuspended in nuclear lysis buffer (50 mM HEPES pH7.5, 150 mM NaCl, 1 mM EDTA, 0.1% Triton X-100, 10% glycerol, 1% SDS, 1× proteinase inhibitor cocktail), then the chromatin was ultrasonically fragmented on ice to an average size of 500 bp. Immunoprecipitations were performed with an anti-GFP beads (MBL, M153-10) overnight at 4 °C. The immunocomplex was successively washed by low-salt wash buffer (50 mM HEPES pH7.5, 150 mM NaCl, 1 mM EDTA), high-salt wash buffer (50 mM HEPES pH7.5, 500 mM NaCl, 1 mM EDTA), LiCl wash buffer (0.25 M LiCl, 0.5% NP-40, 1 mM EDTA, and 10 mM Tris·HCl pH 8.0), and TE buffer (10 mM Tris·HCl pH 8.0 and 1 mM EDTA) and then was eluted with elution buffer (1% SDS and 0.1 M $NaHCO_3$). The DNA fragments were resuspended in sterilized water for qPCR. qPCR was performed using TB Green Premix Ex TaqII (TaKaRa) and LightCycler96 (Roche). KN199 was used as the negative control. The percentage of IP DNA to its corresponding input DNA was represented as enrichment for each target. Relevant primer sequences were listed in Supplementary Data Set 1.

Quantitative analysis of endogenous GAs

Quantification of GAs in the WSB, *wm164*, KN199, Q and Q^{G229S} overexpression wheat was performed as described previously with 3 biological replicates (Liu et al. 2012). At W3.5 stage, 1 g of mixed spike and peduncle tissues was collected separately from WSB, *wm164*, KN199, Q and Q^{G229S} overexpression wheat plants. Samples were immediately ground into powder in liquid nitrogen, then homogenized in 1 mL of 70% methanol by vortexing. The mixture was incubated at 4 °C with vortexing every 10 min for 3 cycles, followed by overnight incubation at 4 °C. The $^2H_2$-GA_1, $^2H_2$-GA_4, $^2H_2$-GA_{19}, $^2H_2$-GA_{20} as internal standards. UPLC-MS/MS analysis was performed using purified extracts on an ABI 4000Q-TRAR LC-MS system (Applied Biosystems, USA).

Statistical analysis

Student's *t*-tests were performed using Microsoft Office Excel; ANOVA analyses were performed using the GraphPad Prism 9.0.

Statistical analyses with *P*-values can be found in Supplementary Data Set 2.

Accession numbers

Sequence data from this study can be found in the WheatOmics 1.0 (http://wheatomics.sdau.edu.cn) under the following accession numbers: Q (*AP2L5*): *TraesCS5A03G1116700*; *q*: *TraesCS5D03G1069300*; *Rht1*: *TraesCS4A03G0701300*; *GID1*:*TraesCS1A03G0655800*; *GID2*: *TraesCS3A03G0116000*; *GA3ox2*: *TraesCS3A03G0268400*, *TraesCS3B03G0336700*, *TraesCS3D03G0261200*; *KS1*: *TraesCS2A03G1015500*, *TraesCS2B03G1337500*, *TraesCS2D03G0955700*; *KO2*: *TraesCS7A03G0885500*, *TraesCS7B03G0729700*, *TraesCS7D03G0850500*; *GA20ox1*: *TraesCS4A03G0796400*, *TraesCS5B03G1356500*, *TraesCS5D03G1210400*; *GA20ox2*: *TraesCS3A03G0950800*, *TraesCS3B03G1087000*, *TraesCS3D03G0884400*; *GA20ox3*: *TraesCS3A03G0937900*, *TraesCS3B03G1067800*, *TraesCS3D03G0870200*; *GAPDH*: *TraesCS6A03G0586800*, *TraesCS6B03G0715800*, *TraesCS6D03G0485700*.

Acknowledgments

We would like to thank professor Kong Xiuying and Zheng Lingli for performing the wheat transformation.

Author contributions

J.J., X.L., L.G., Z.L., and P.L. designed experiments and drafted the initial article; P.L., S.X., L.G., and Z.L. performed most of the experiments; G.Z., J.L., and H.W. analyzed the data; Y.H., C.K., and D.Y. contributed to traits collection. All authors discussed the results, reviewed the article, and approved the final article.

Supplementary data

The following materials are available in the online version of this article.

Supplementary Figure S1. Phenotypes of the *wm164* mutant and mapping of *QSpl*-5A (supports Fig. 1).

Supplementary Figure S2. Fine mapping of *QSpl*-5A using the *mw164*×WSB BC_2F_2 population (supports Fig. 1).

Supplementary Figure S3. Comparison of the protein sequences, 2D and 3D structural models of Q and Q^{G229S} (supports Fig. 1).

Supplementary Figure S4. Phenotypes of KN199, *pUbi*:Q, *pUbi*:Q^{G229S}, and *KO*-5AQ transgenic wheat (supports Fig. 1).

Supplementary Figure S5. The AP2 domain and C terminus of Q mediate homodimer formation (supports Fig. 2).

Supplementary Figure S6. Q represses GA biosynthesis by directly targeting *GA3ox2* (supports Fig. 3).

Supplementary Figure S7. Q protein abundance is not affected by GA_3 treatment and Q directly interacts with RHT1 and GID2 (supports Fig. 4).

Supplementary Figure S8. Q restrict plant height and spike length by blocking the GID2–RHT1 interaction (supports Fig. 4).

Supplementary Table S1. The plant height and spike length of *pUbi*:Q, *pUbi*:Q^{G229S}, pUbi:GA3ox2, *pUbi*:Q/*pUbi*:*GA3ox2*, *pUbi*:Q^{G229S}/*pUbi*:*GA3ox2*, and *KO*-5AQ transgenic wheat lines.

Supplementary Table S2. The genotypes of 16 recombinants identified between markers *CAPS64910* and *CAPS655070* and their phenotypes.

Supplementary Table S3. Thirty-three high-confidence genes annotated within the 1.41-Mb *SNP65131-CAPS65272* interval.

Supplementary Table S4. Twenty SNPs identified within the 1.41-Mb target interval through re-sequencing of WSB and *mw164*.

Supplementary Table S5. Mean spike length (SPL) of plants with identical *Kasp*-Q genotypes in the (*mw164* × ND2419) F_2 population and the (*mw164* × WSB) BC_2F_2 population.

Supplementary Data Set 1. Primers used in this study.

Supplementary Data Set 2. Results of the Student's t-tests and 1/2-way ANOVA analyses conducted in this study.

Funding

This study was partially supported by Natural Science Foundation of China (31991213, 32201750), Key Technology Research and Development Program of Henan Province of China (232102111079, 225200810024, 231111112900, and 241111110900), Opening Foundation of National Key Laboratory of Wheat Improvement (WIKF202404), the Outstanding Young Scientist Foundation of NSFC (Overseas), Innovation Program of Chinese Academy of Agricultural Sciences, and Chinese Academy of Agricultural Sciences Young Talent Scientist Program.

Conflict of interest statement. None declared.

Data availability

The data underlying this article are available in the article and in its online Supplementary material.

References

Binenbaum J, Weinstain R, Shani E. Gibberellin localization and transport in plants. *Trends Plant Sci*. 2018:23(5):410–421. https://doi.org/10.1016/j.tplants.2018.02.005

Chen H, Zou Y, Shang Y, Lin H, Wang Y, Cai R, Tang X, Zhou J-M. Firefly luciferase complementation imaging assay for protein-protein interactions in plants. *Plant Physiol*. 2008:146(2):368–376. https://doi.org/10.1104/pp.107.111740

Chen Q, Guo Z, Shi X, Wei M, Fan Y, Zhu J, Zheng T, Wang Y, Kong L, Deng M, et al. Increasing the grain yield and grain protein content of common wheat (*Triticum aestivum*) by introducing missense mutations in the Q gene. *Int J Mol Sci*. 2022:23(18):10772. https://doi.org/10.3390/ijms231810772

Chen SL, Gao G, Wang HY, Wen MX, Xiao J, Bian N, Zhang RQ, Hu WJ, Cheng SH, Wang X, et al. Characterization of a novel reduced height gene (*Rht23*) regulating panicle morphology and plant architecture in bread wheat. *Euphytica*. 2015:203(3):583–594. https://doi.org/10.1007/s10681-014-1275-1

Chen Y, Chen Y, Shi C, Huang Z, Zhang Y, Li S, Li Y, Ye J, Yu C, Li Z, et al. SOAPnuke: a MapReduce acceleration-supported software for integrated quality control and preprocessing of high-throughput sequencing data. *Gigascience*. 2018:7(1):1–6. https://doi.org/10.1093/gigascience/gix120

Cheng X, Zhang S, Tao W, Zhang X, Liu J, Sun J, Zhang H, Pu L, Huang R, Chen T. Indeterminate spikelet1 recruits histone deacetylase and a transcriptional repression complex to regulate rice salt tolerance. *Plant Physiol*. 2018:178(2):824–837. https://doi.org/10.1104/pp.18.00324

Chiang HH, Hwang I, Goodman HM. Isolation of the Arabidopsis GA4 locus. *Plant Cell*. 1995:7(2):195–201. https://doi.org/10.1105/tpc.7.2.195

Debernardi JM, Lin H, Chuck G, Faris JD, Dubcovsky J. microRNA172 plays a crucial role in wheat spike morphogenesis and grain threshability. *Development*. 2017:144(11):1966–1975. https://doi.org/10.1242/dev.146399

Dill A, Thomas SG, Hu J, Steber CM, Sun TP. The Arabidopsis F-box protein SLEEPY1 targets gibberellin signaling repressors for

gibberellin-induced degradation. *Plant Cell*. 2004:16(6):1392–1405. https://doi.org/10.1105/tpc.020958

Fleet CM, Yamaguchi S, Hanada A, Kawaide H, David CJ, Kamiya Y, Sun TP. Overexpression of *AtCPS* and *AtKS* in Arabidopsis confers increased *ent*-kaurene production but no increase in bioactive gibberellins. *Plant Physiol*. 2003:132(2):830–839. https://doi.org/10.1104/pp.103.021725

Flintham JE, Borner A, Worland AJ, Gale MD. Optimizing wheat grain yield: effects of *Rht* (gibberellin-insensitive) dwarfing genes. *J Agric Sci*. 1997:128(1):11–25. https://doi.org/10.1017/S0021859696003942

Fu X, Richards DE, Fleck B, Xie D, Burton N, Harberd NP. The Arabidopsis mutant sleepy1^{gar2-1} protein promotes plant growth by increasing the affinity of the SCF^{SLY1} E3 ubiquitin ligase for DELLA protein substrates. *Plant Cell*. 2004:16(6):1406–1418. https://doi.org/10.1105/tpc.021386

Gendrel AV, Lippman Z, Martienssen R, Colot V. Profiling histone modification patterns in plants using genomic tiling microarrays. *Nat Methods*. 2005:2(3):213–218. https://doi.org/10.1038/nmeth0305-213

Greenwood JR, Finnegan EJ, Watanabe N, Trevaskis B, Swain SM. New alleles of the wheat domestication gene Q reveal multiple roles in growth and reproductive development. *Development*. 2017:144(11):1959–1965. https://doi.org/10.1242/dev.146407

Guo Z, Chen Q, Zhu J, Wang Y, Li Y, Li Q, Zhao K, Li Y, Tang R, Shi X, et al. The Q^{c5} allele increases wheat bread-making quality by regulating SPA and SPR. *Int J Mol Sci*. 2022:23(14):7581. https://doi.org/10.3390/ijms23147581

Harberd NP, Belfield E, Yasumura Y. The angiosperm gibberellin-GID1-DELLA growth regulatory mechanism: how an "inhibitor of an inhibitor" enables flexible response to fluctuating environments. *Plant Cell*. 2009:21(5):1328–1339. https://doi.org/10.1105/tpc.109.066969

He G, Zhang Y, Liu P, Jing Y, Zhang L, Zhu Y, Kong X, Zhao H, Zhou Y, Sun J. The transcription factor TaLAX1 interacts with Q to antagonistically regulate grain threshability and spike morphogenesis in bread wheat. *New Phytol*. 2021:230(3):988–1002. https://doi.org/10.1111/nph.17235

Hellens RP, Allan AC, Friel EN, Bolitho K, Grafton K, Templeton MD, Karunairetnam S, Gleave AP, Laing WA. Transient expression vectors for functional genomics, quantification of promoter activity and RNA silencing in plants. *Plant Methods*. 2005:1(1):13. https://doi.org/10.1186/1746-4811-1-13

Helliwell CA, Chandler PM, Poole A, Dennis ES, Peacock WJ. The CYP88A cytochrome P450, *ent*-kaurenoic acid oxidase, catalyzes three steps of the gibberellin biosynthesis pathway. *Proc Natl Acad Sci U S A*. 2001:98(4):2065–2070. https://doi.org/10.1073/pnas.98.4.2065

Hu J, Mitchum MG, Barnaby N, Ayele BT, Ogawa M, Nam E, Lai WC, Hanada A, Alonso JM, Ecker JR, et al. Potential sites of bioactive gibberellin production during reproductive growth in Arabidopsis. *Plant Cell*. 2008:20(2):320–336. https://doi.org/10.1105/tpc.107.057752

Huang X, Zeller FJ, Hsam SL, Wenzel G, Mohler V. Chromosomal location of AFLP markers in common wheat utilizing nulli-tetrasomic stocks. *Genome*. 2000:43(2):298–305. https://doi.org/10.1139/g99-118

International Wheat Genome Sequencing Consortium (IWGSC). Shifting the limits in wheat research and breeding using a fully annotated reference genome. *Science*. 2018:361(6403):eaar7191. https://doi.org/10.1126/science.aar7191

Ishida Y, Tsunashima M, Hiei Y, Komari T. Wheat (*Triticum aestivum* L.) transformation using immature embryos. *Methods Mol Biol*. 2015:1223:89–198. https://doi.org/10.1007/978-1-4939-1695-5_15

Jiang YF, Chen Q, Wang Y, Guo ZR, Xu BJ, Zhu J, Zhang YZ, Gong X, Luo CH, Wu W, et al. Re-acquisition of the brittle rachis trait via a transposon insertion in domestication gene Q during wheat de-domestication. *New Phytol*. 2019:224(2):961–973. https://doi.org/10.1111/nph.15977

Laemmli UK. Cleavage of structural proteins during the assembly of the head of bacteriophage T4. *Nature*. 1970:227(5259):680–685. https://doi.org/10.1038/227680a0

Li H, Durbin R. Fast and accurate short read alignment with Burrows-Wheeler transform. *Bioinformatics*. 2009:25(14):1754–1760. https://doi.org/10.1093/bioinformatics/btp324

Lin Q, Jin S, Zong Y, Yu H, Zhu Z, Liu G, Kou L, Wang Y, Qiu JL, Li J, et al. High-efficiency prime editing with optimized, paired pegRNAs in plants. *Nat Biotechnol*. 2021:39(8):923–927. https://doi.org/10.1038/s41587-021-00868-w

Liu H, Li X, Xiao J, Wang S. A convenient method for simultaneous quantification of multiple phytohormones and metabolites: application in study of rice-bacterium interaction. *Plant Methods*. 2012:8(1):2. https://doi.org/10.1186/1746-4811-8-2

Liu P, Liu J, Dong H, Sun J. Functional regulation of Q by microRNA172 and transcriptional co-repressor TOPLESS in controlling bread wheat spikelet density. *Plant Biotechnol J*. 2018:16(2):495–506. https://doi.org/10.1111/pbi.12790

Ma Z, Wu T, Huang K, Jin YM, Li Z, Chen M, Yun S, Zhang H, Yang X, Chen H, et al. A novel AP2/ERF transcription factor, OsRPH1, negatively regulates plant height in rice. *Front Plant Sci*. 2020:11:709. https://doi.org/10.3389/fpls.2020.00709

Madsen CK, Brinch-Pedersen H. A novel wheat *q'* allele identified by forward genetic in silico TILLING. *J Plant Physiol*. 2020:251:153221. https://doi.org/10.1016/j.jplph.2020.153221

Magome H, Nomura T, Hanada A, Takeda-Kamiya N, Ohnishi T, Shinma Y, Katsumata T, Kawaide H, Kamiya Y, Yamaguchi S. *CYP714B1* and *CYP714B2* encode gibberellin 13-oxidases that reduce gibberellin activity in rice. *Proc Natl Acad Sci U S A*. 2013:110(5):1947–1952. https://doi.org/10.1073/pnas.1215788110

McKenna A, Hanna M, Banks E, Sivachenko A, Cibulskis K, Kernytsky A, Garimella K, Altshuler D, Gabriel S, Daly M, et al. The Genome analysis toolkit: a MapReduce framework for analyzing next-generation DNA sequencing data. *Genom Res*. 2010:20(9):1297–1303. https://doi.org/10.1101/gr.107524.110

Muramatsu M. Dosage effect of the spelta gene *q* of hexaploid wheat. *Genetics*. 1963:48(4):469–482. https://doi.org/10.1093/genetics/48.4.469

Murase K, Hirano Y, Sun TP, Hakoshima T. Gibberellin-induced DELLA recognition by the gibberellin receptor GID1. *Nature*. 2008:456(7221):459–463. https://doi.org/10.1038/nature07519

Ni P, Zhao Y, Zhou X, Liu Z, Huang Z, Ni Z, Sun Q, Zong Y. Efficient and versatile multiplex prime editing in hexaploid wheat. *Genome Biol*. 2023:24(1):156. https://doi.org/10.1186/s13059-023-02990-1

Niu L, Lin H, Zhang F, Watira TW, Li G, Tang Y, Wen J, Ratet P, Mysore KS, Tadege M. *LOOSE FLOWER*, a *WUSCHEL*-like Homeobox gene, is required for lateral fusion of floral organs in *Medicago truncatula*. *Plant J*. 2015:81(3):480–492. https://doi.org/10.1111/tpj.12743

Okamuro JK, Caster B, Villarroel R, Van Montagu M, Jofuku KD. The AP2 domain of APETALA2 defines a large new family of DNA binding proteins in Arabidopsis. *Proc Natl Acad Sci U S A*. 1997:94(13):7076–7081. https://doi.org/10.1073/pnas.94.13.7076

Patil V, McDermott HI, McAllister T, Cummins M, Silva JC, Mollison E, Meikle R, Morris J, Hedley PE, Waugh R, et al. APETALA2 control of barley internode elongation. *Development*. 2019:146(11): dev170373. https://doi.org/10.1242/dev.170373

Peng J, Richards DE, Hartley NM, Murphy GP, Devos KM, Flintham JE, Beales J, Fish LJ, Worland AJ, Pelica F, et al. 'Green revolution' genes encode mutant gibberellin response modulators. *Nature*. 1999:400(6741):256–261. https://doi.org/10.1038/22307

Phillips AL, Ward DA, Uknes S, Appleford NE, Lange T, Huttly AK, Gaskin P, Graebe JE, Hedden P. Isolation and expression of three gibberellin 20-oxidase cDNA clones from Arabidopsis. *Plant Physiol*. 1995:108(3):1049–1057. https://doi.org/10.1104/pp.108.3.1049

Sasaki A, Ashikari M, Ueguchi-Tanaka M, Itoh H, Nishimura A, Swapan D, Ishiyama K, Saito T, Kobayashi M, Khush GS, et al. Green revolution: a mutant gibberellin-synthesis gene in rice. *Nature*. 2002:416(6882):701–702. https://doi.org/10.1038/416701a

Sasaki A, Itoh H, Gomi K, Ueguchi-Tanaka M, Ishiyama K, Kobayashi M, Jeong DH, An G, Kitano H, Ashikari M, et al. Accumulation of phosphorylated repressor for gibberellin signaling in an F-box mutant. *Science*. 2003:299(5614):1896–1898. https://doi.org/10.1126/science.1081077

Shimada A, Ueguchi-Tanaka M, Nakatsu T, Nakajima M, Naoe Y, Ohmiya H, Kato H, Matsuoka M. Structural basis for gibberellin recognition by its receptor GID1. *Nature*. 2008:456(7221): 520–523. https://doi.org/10.1038/nature07546

Simons KJ, Fellers JP, Trick HN, Zhang Z, Tai YS, Gill BS, Faris JD. Molecular characterization of the major wheat domestication gene Q. *Genetics*. 2006:172(1):547–555. https://doi.org/10.1534/genetics.105.044727

Song L, Liu J, Cao B, Liu B, Zhang X, Chen Z, Dong C, Liu X, Zhang Z, Wang W, et al. Reducing brassinosteroid signalling enhances grain yield in semi-dwarf wheat. *Nature*. 2023:617(7959): 118–124. https://doi.org/10.1038/s41586-023-06023-6

Sun T, Goodman HM, Ausubel FM. Cloning the Arabidopsis *GA1* locus by genomic subtraction. *Plant Cell*. 1992:4(2):119–128. https://doi.org/10.2307/3869565

Ueguchi-Tanaka M, Ashikari M, Nakajima M, Itoh H, Katoh E, Kobayashi M, Chow TY, Hsing YI, Kitano H, Yamaguchi I, et al. *GIBBERELLIN INSENSITIVE DWARF1* encodes a soluble receptor for gibberellin. *Nature*. 2005:437(7059):693–698. https://doi.org/10.1038/nature04028

Varbanova M, Yamaguchi S, Yang Y, McKelvey K, Hanada A, Borochov R, Yu F, Jikumaru Y, Ross J, Cortes D, et al. Methylation of gibberellins by Arabidopsis GAMT1 and GAMT2. *Plant Cell*. 2007:19(1):32–45. https://doi.org/10.1105/tpc.106.044602

Wang K, Li M, Hakonarson H. ANNOVAR: functional annotation of genetic variants from high-throughput sequencing data. *Nucleic Acids Res*. 2010:38(16):e164. https://doi.org/10.1093/nar/gkq603

Wang K, Shi L, Liang X, Zhao P, Wang W, Liu J, Chang Y, Hiei Y, Yanagihara C, Du L, et al. The gene *TaWOX5* overcomes genotype dependency in wheat genetic transformation. *Nat Plants*. 2022:8(2):110–117. https://doi.org/10.1038/s41477-021-01085-8

Wu K, Xu H, Gao X, Fu X. New insights into gibberellin signaling in regulating plant growth-metabolic coordination. *Curr Opin Plant Biol*. 2021:63:102074. https://doi.org/10.1016/j.pbi.2021.102074

Xie Q, Li N, Yang Y, Lv Y, Yao H, Wei R, Sparkes DL, Ma Z. Pleiotropic effects of the wheat domestication gene Q on yield and grain morphology. *Planta*. 2018:247(5):1089–1098. https://doi.org/10.1007/s00425-018-2847-4

Xing H-L, Dong L, Wang Z-P, Zhang H-Y, Han C-Y, Liu B, Wang X-C, Chen Q-J. A CRISPR/Cas9 toolkit for multiplex genome editing in plants. *BMC Plant Biol*. 2014:14(1):327. https://doi.org/10.1186/s12870-014-0327-y

Xu B-J, Chen Q, Zheng T, Jiang Y-F, Qiao Y-Y, Guo Z-R, Cao Y-L, Wang Y, Zhang Y-Z, Zong L-J, et al. An overexpressed Q allele leads to increased spike density and improved processing quality in common wheat (*Triticum aestivum* L). *G3*. 2018:8(3):771–778. https://doi.org/10.1534/g3.117.300562

Xu D, Bian Y, Luo X, Jia C, Hao Q, Tian X, Cao Q, Chen W, Ma W, Ni Z, et al. Dissecting pleiotropic functions of the wheat Green Revolution gene *Rht-B1b* in plant morphogenesis and yield formation. *Development*. 2023:150(20):dev201601. https://doi.org/10.1242/dev.201601

Yaish MW, El-Kereamy A, Zhu T, Beatty PH, Good AG, Bi YM, Rothstein SJ. The APETALA-2-like transcription factor OsAP2-39 controls key interactions between abscisic acid and gibberellin in rice. *PLoS Genet*. 2010:6(9):e1001098. https://doi.org/10.1371/journal.pgen.1001098

Yamaguchi S, Sun T-p, Kawaide H, Kamiya Y. The *GA2* locus of Arabidopsis thaliana encodes *ent*-kaurene synthase of gibberellin biosynthesis. *Plant Physiol*. 1998:116(4):1271–1278. https://doi.org/10.1104/pp.116.4.1271

Yang Z, Yang R, Bai W, Chen W, Kong X, Zhou Y, Qiao W, Zhang Y, Sun J. Q negatively regulates wheat salt tolerance through directly repressing the expression of *TaSOS1* and reactive oxygen species scavenging genes. *Plant J*. 2024:119(1):478–489. https://doi.org/10.1111/tpj.16777

Zhang C, Gao L, Sun J, Jia J, Ren Z. Haplotype variation of Green Revolution gene *Rht-D1* during wheat domestication and improvement. *J Integr Plant Biol*. 2014:56(8):774–780. https://doi.org/10.1111/jipb.12197

Zhang J, Xiong H, Guo H, Li Y, Xie X, Xie Y, Zhao L, Gu J, Zhao S, Ding Y, et al. Identification of the Q gene playing a role in spike morphology variation in wheat mutants and its regulatory network. *Front Plant Sci*. 2022:12:807731. https://doi.org/10.3389/fpls.2021.807731

Zhang Z, Belcram H, Gornicki P, Charles M, Just J, Huneau C, Magdelenat G, Couloux A, Samain S, Gill BS, et al. Duplication and partitioning in evolution and function of homoeologous Q loci governing domestication characters in polyploid wheat. *Proc Natl Acad Sci U S A*. 2011:108(46):18737–18742. https://doi.org/10.1073/pnas.1110552108

Zhang Z, Li A, Song G, Geng S, Gill BS, Faris JD, Mao L. Comprehensive analysis of Q gene near-isogenic lines reveals key molecular pathways for wheat domestication and improvement. *Plant J*. 2020:102(2):299–310. https://doi.org/10.1111/tpj.14624

Zhao K, Xiao J, Liu Y, Chen S, Yuan C, Cao A, You FM, Yang D, An S, Wang H, et al. *Rht23* (*5Dq'*) likely encodes a Q homeologue with pleiotropic effects on plant height and spike compactness. *Theor Appl Genet*. 2018:131(9):1825–1834. https://doi.org/10.1007/s00122-018-3115-5

Zhu T, Wang L, Rimbert H, Rodriguez JC, Deal KR, De Oliveira R, Choulet F, Keeble-Gagnère G, Tibbits J, Rogers J, et al. Optical maps refine the bread wheat *Triticum aestivum* cv. Chinese Spring genome assembly. *Plant J*. 2021:107(1):303–314. https://doi.org/10.1111/tpj.15289